

# Ferromagnetic ordering and magnetic anisotropy of a Mn monolayer on Nb(001)

Jisang Hong

Department of Physics, Pukyong National University, Busan 608-737, Korea

R. Q. Wu

Department of Physics and Astronomy, University of California, Irvine, California 92697, USA

(Received 24 January 2006; published 30 March 2006)

Through density functional full-potential linearized augmented-plane-wave calculations, we found that it is possible to materialize a ferromagnetic Mn monolayer on nonmagnetic Nb(001). It was obtained that the surface Nb atom has a large induced magnetic moment of  $-0.56\mu_B$  and the Nb has an antiferromagnetic exchange interaction with the Mn adlayer. We attribute this antiferromagnetic exchange interaction between Mn and Nb atoms to the realization of a ferromagnetic ground state in a Mn monolayer on the Nb(001) surface. We also present the calculated results of x-ray magnetic circular dichroism and magnetic anisotropy. It was observed that Mn/Nb(001) has weak perpendicular magnetocrystalline anisotropy, but the easy axis is in plane due to the shape anisotropy.

DOI: [10.1103/PhysRevB.73.094450](https://doi.org/10.1103/PhysRevB.73.094450)

PACS number(s): 75.30.Gw, 75.75.+a

## I. INTRODUCTION

Low-dimensional magnetic materials furnish many important properties for both fundamental investigations and innovative device applications.<sup>1</sup> Among  $3d$  elements, Mn is particularly interesting due to its large local magnetic moment when it is used as a dopant or adsorbate. Properties of Mn thin films on both magnetic and nonmagnetic substrates have been extensively investigated.<sup>2-4</sup> Typically, Mn tends to adopt antiferromagnetic (AF) ordering, regardless of the magnetic features of the substrate. For instance, Mn monolayers form a  $c(2 \times 2)$  AF structure on the Fe substrate as was revealed both theoretically and experimentally.<sup>5,6</sup> Although it was reported that the Mn monolayer displays ferromagnetic (FM) behavior in Mn/Ni(001) (Ref. 7) and Mn/Co(001),<sup>8</sup> the results are controversial and the involvement of O was introduced to explain the discrepancy between theory and experiment.<sup>9</sup> Until recently, no-one has reported a FM ground state of a Mn monolayer on nonmagnetic substrate materials despite the fact that extensive explorations have been done.<sup>10-13</sup> On the other hand, FM ordering between Mn atoms was found in surface alloys, such as MnCo/Cu(001),<sup>14</sup> MnNi/Ni(001), and MnCu/Cu(001).<sup>7</sup> In addition, small Mn clusters,<sup>15</sup> wires,<sup>16</sup> and dimers<sup>17</sup> are ferromagnetic in certain geometries. It was found in our recent calculations that a  $\delta$ -doped Mn monolayer in GaAs also has a stable in-plane FM ground state.<sup>18</sup> Very interestingly, it was presented through first principles calculations that a pure Mn monolayer (ML) can have a ferromagnetic ground state on a W(001) surface.<sup>19</sup>

To further investigate the mechanism that governs magnetic ordering between Mn atoms in different environments, we explored magnetic ordering of Mn on various substrates. Here we report results of density functional calculations that a Mn monolayer is ferromagnetic on Nb(001), primarily driven by the strong induced magnetization in the substrate. After a brief description of computational details in Sec. II, we discuss results of magnetic ordering, magnetic anisotropy, and magnetic circular dichroism in Sec. III, and provide concluding statements in Sec. IV.

## II. NUMERICAL METHOD

An isolated seven-layer slab of five Nb and two Mn layers was used to simulate the Mn/Nb(001) system. Mn atoms were placed pseudomorphically on the fourfold hollow sites above Nb(001). The lattice constant in the lateral plane was taken from experimental data for the bulk bcc Nb, 6.238 a.u. The vertical positions of all the atoms were optimized through the total energy minimization procedure guided by the calculated atomic forces. We explored the FM,  $p(2 \times 1)$  AF, and  $c(2 \times 2)$  AF configurations and thus different two-dimensional unit cells were employed. The convergence of electronic and magnetic properties against computational parameters was carefully checked.

The thin film version of the all-electron full-potential linearized augmented-plane-wave (FLAPW) method was adopted.<sup>20</sup> There is thereby no shape approximation in charge, potential and wave function expansions. In the FLAPW calculations, energy cutoffs of 225 and 13.7 Ry were chosen for the charge or potential and basis expansions in the interstitial region. Spherical harmonics with a maximum angular momentum quantum number of  $l_{max}=8$  were

TABLE I. The calculated magnetic moment  $M$  (in  $\mu_B$ ) and vertical positions  $z$  (in a.u.) of Mn and surface Nb(s) atom.

System		Mn	Nb(s)	$E$
$p(2 \times 1)$	$M_{AFM}$	$\pm 3.30$	0	151.41
	$z$	8.99	6.371	
$c(2 \times 2)$	$M_{AFM}$	$\pm 3.48$	0	458.09
	$z$	9.12	6.371	
$p(1 \times 1)$	$M_{FM}$	3.23	-0.56	0
	$z$	8.97	6.371	

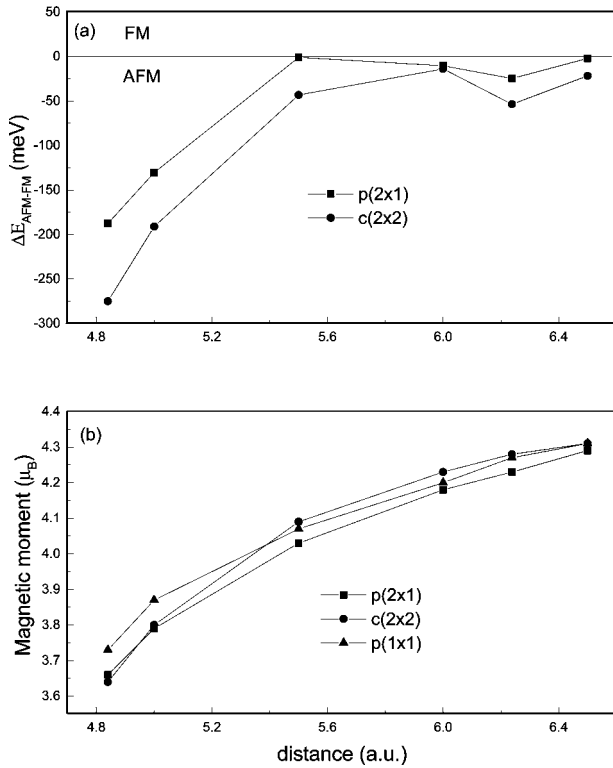


FIG. 1. (a) Calculated energy difference  $\Delta E_{AFM-FM}$  and (b) magnetic moments as a function of lattice size.

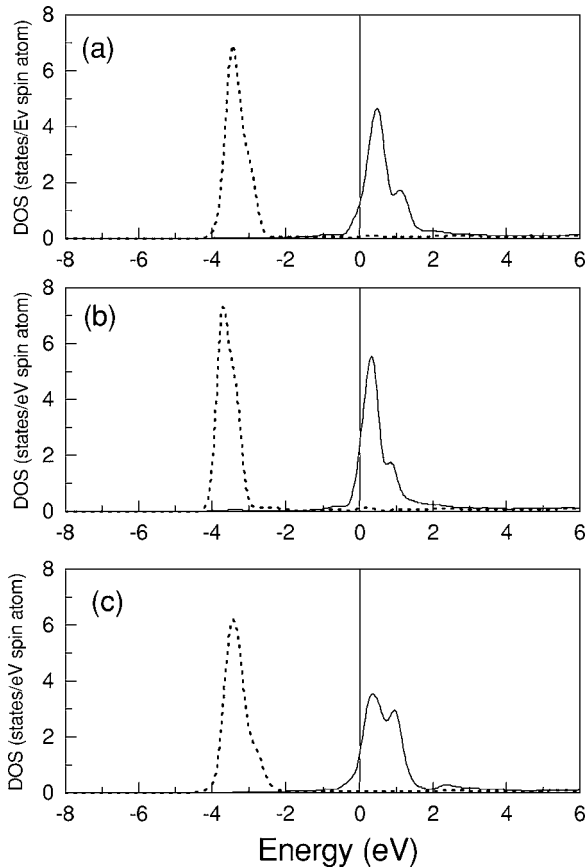


FIG. 2. Spin-polarized DOS of Mn in free-standing case: (a)  $p(2 \times 1)$  AFM, (b)  $c(2 \times 2)$  AFM, and (c) FM.

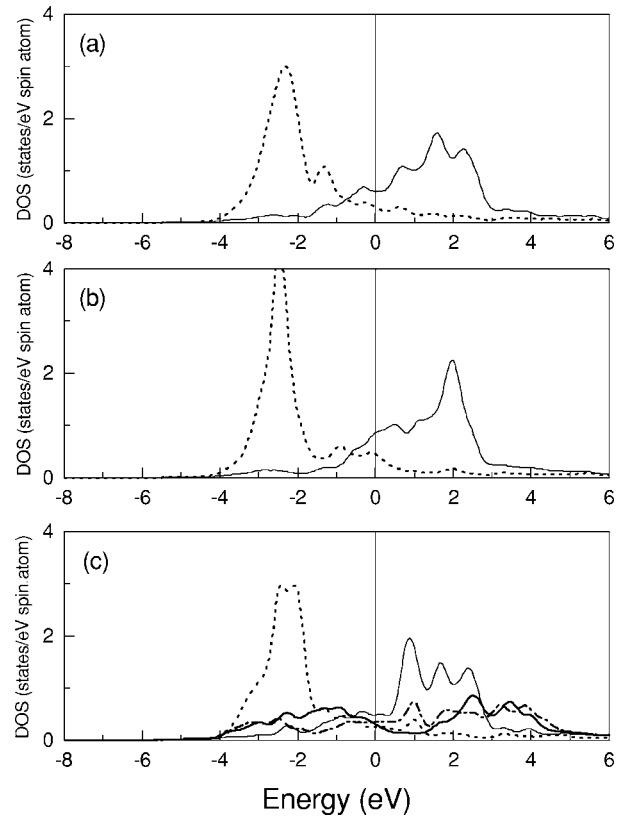


FIG. 3. Spin-polarized DOS of Mn ML on Nb(001) surface: (a)  $p(2 \times 1)$  AFM, (b)  $c(2 \times 2)$  AFM, and (c) FM and the low-lying states are for the surface Nb atom (thick dash-dot for spin up and thick solid line for spin down).

used for all the expansions in the muffin-tin region. The generalized gradient approximation<sup>21</sup> was adopted to describe the exchange-correlation interaction. We used 120  $k$  points in the irreducible two-dimensional Brillouin zone to evaluate integrals in the reciprocal space.

### III. NUMERICAL RESULTS AND DISCUSSIONS

It is known that a well-optimized atomic structure is crucial for the determination of magnetic ordering in Mn layers. Through the total energy minimization procedure, we found that the Mn-Nb( $s$ ) interlayer distance varies in different magnetic configurations. As listed in Table I, the equilibrium interlayer distances between Mn and Nb( $s$ ) are 2.619, 2.749, and 2.599 a.u. in the  $p(2 \times 1)$  AF,  $c(2 \times 2)$  AF, and FM states, respectively. On the other side, the presence of Mn causes a 2% expansion in the substrate. Strikingly, despite strong Mn-Nb hybridization, the local magnetic moments of Mn remain large, e.g.,  $3.23 \mu_B$  in the FM phase. Interestingly, the FM Mn adlayer induces a large negative magnetic moment in Nb( $s$ ),  $-0.56 \mu_B$ .

Total energy calculations revealed that the FM state instead of the  $c(2 \times 2)$  AFM state is the preferred phase in Mn/Nb(001). Experimental verifications are desired for this important theoretical prediction. In Practice, one may question whether it is possible to materialize this system due to

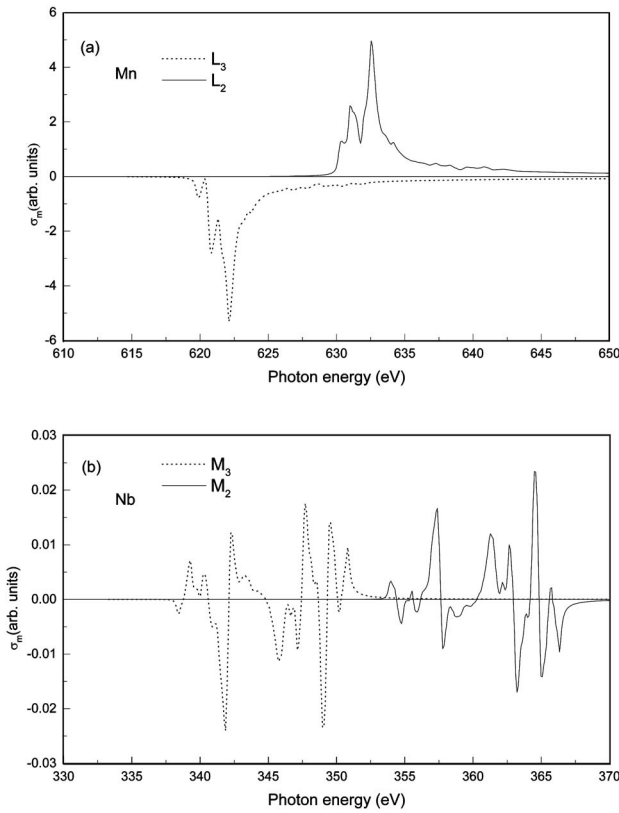


FIG. 4. XMCD spectra of (a) Mn and (b) Nb.

(1) the large lattice mismatch and (2) possible surface interdiffusion or the formation of complex surface alloys. To answer these questions, it is known that most metal layers grow pseudomorphically in the ultrathin regime if the adsorbate-substrate interaction is strong. For Mn/Nb(001), we found that the adsorption energy [defined as the energy difference between Mn/Nb(001), the clean Nb(001) surface, and the free pseudomorphic Mn monolayer] is very large, 2.86 eV per Mn atom. Furthermore, the mixed structure with two 50-50 Mn-Nb alloy layers is 0.12 eV higher in energy than the case with a sharp Mn/Nb(001) interface. We hence believe that it is feasible to grow a flat Mn monolayer on Nb(001) experimentally.

To reveal if the FM ground state in Mn/Nb(001) is produced by lattice expansion or by adlayer-substrate hybridization, we also studied the free-standing square Mn monolayer with a varying lattice size. The calculated energy differences (defined as  $\Delta E_{AFM-FM}$ ) and magnetic moments for unsupported structures are presented in Fig. 1. One can clearly see that the  $c(2 \times 2)$  AFM state is the stable ground state in a wide range of lattice size. When the lattice matches the Nb(001) substrate ( $a=6.228$  a.u.), surprisingly, the energy ordering for different magnetic states in the free Mn ML is reversed from that in Mn/Nb(001). This clearly indicates that the FM ordering in Mn/Nb(001) stems from the Mn-Nb hybridization, rather than the lattice expansion. This differs from the trend observed from previous studies that strong overlayer-substrate hybridization promotes AFM ordering.<sup>1</sup> The large negative magnetic moment induced in the Nb sur-

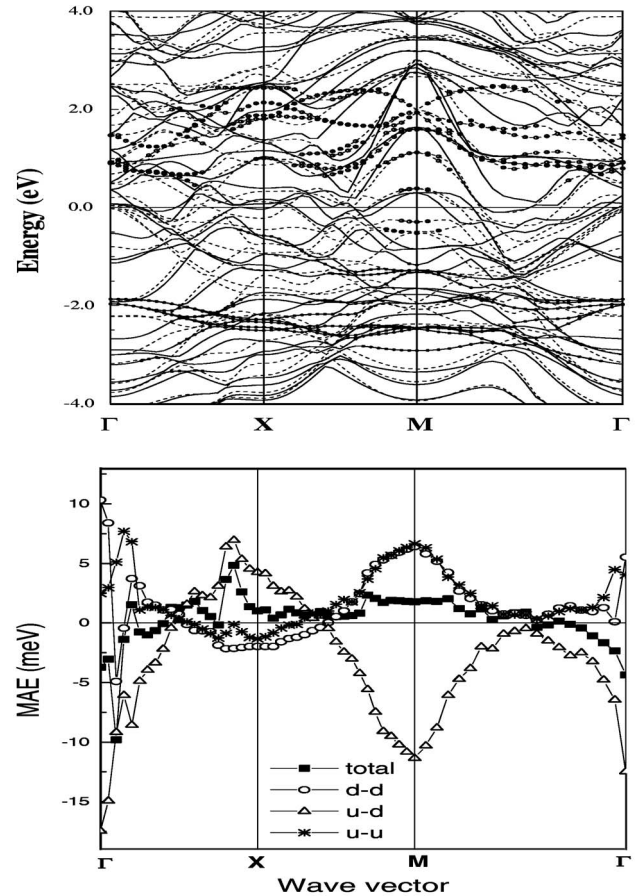


FIG. 5. Magnetocrystalline anisotropy energy distribution and band structures along the high-symmetry directions in two-dimensional Brillouin zone.

face atom plays an essential role in the ferromagnetism of Mn MLs since the AFM Mn layer diminishes the net magnetization entirely. The local magnetic moment of Mn is generally large, almost independent of the change in magnetic ordering. In addition, we found that the orbital magnetic moments are very small [about  $(0.02-0.03)\mu_B$  in a free Mn ML and 0.001 in Mn/Nb(001)].

The density of states (DOS) for the free and supported Mn MLs are plotted in Figs. 2 and 3. For the free Mn ML ( $a=6.228$  a.u.), the majority spin band is far below the Fermi level, whereas the minority spin band is almost empty. The interaction between Mn atoms is rather weak in such a large lattice, indicated by the narrow DOS curves as well as by the negligible resonance between the two sublattices in the AFM states. The majority spin  $d$  band of the  $c(2 \times 2)$  phase is narrower and lower than those in other configurations. In fact, the energy gain from interatomic hybridization is small since the Mn  $d$  shell is fully filled in one spin channel, whereas it remains almost empty in the other spin channel. In Fig. 3, Mn minority spin  $d$  bands are drastically broadened in Mn/Nb(001), especially in the unoccupied region. In contrast, the bandwidth of the majority spin part is much less affected by the presence of the Nb(001) substrate. The FM ordering also appears to reduce the value of DOS at  $E_F$  for

both Mn and Nb(*s*), another reason that stabilizes the FM ordering in Mn/Nb(001).

X-ray magnetic circular dichroism (XMCD) is an ideal technique for verification of our predictions. We present the XMCD spectra for Mn and Nb in Mn/Nb(001) in Fig. 4. Interestingly, the XMCD spectrum for Mn displays three pronounced peaks at both  $L_2$  and  $L_3$  edges, in accordance with the DOS of empty states in Fig. 3. The fine structures should be measurable since their energy separations are quite large (about 1 eV apart). Note the tail of the  $L_3$  edge extends to the region of the  $L_2$  peak. This may cause overestimation in the orbital magnetic moment, which is proportional to the difference between the areas covered by the two edges according to the sum rules.<sup>22,23</sup> The XMCD for the surface Nb atom is strongly oscillatory throughout a wide energy range. Nevertheless, the pronounced negative peak at the  $L_3$  edge, an indication of antiparallel spin alignment, should be detectable.

Magnetic anisotropy is one of the most important properties in dealing with magnetism. We determined the uniaxial component of the magnetocrystalline anisotropy energy  $E_{MCA}$  of Mn/Nb(001) with the torque method.<sup>24</sup> The value of  $E_{MCA}$  is 58  $\mu\text{eV}$  per Mn atom, with an easy axis along the

surface normal. Nonetheless, if one takes into account the shape anisotropy, which is 244  $\mu\text{eV}$  through summing up the discrete dipole contributions, the direction of magnetization of Mn/Nb(001) is expected to lie in plane. To reveal the physics that produces the positive  $E_{MCA}$ , we explored the distribution of  $E_{MCA}$  in the two-dimensional Brillouin zone along with the band structures in Fig. 5. From the curves in the bottom panel, one can see that  $E_{MCA}$  strongly fluctuates along the  $\Gamma$ - $X$  direction and large positive contributions (leading to perpendicular magnetization) are found in most areas of the Brillouin zone except in the vicinity around the  $\Gamma$  point. Overall, there is no “hot”  $k$  point that makes a dominant contribution. Besides, it seems that the largest contribution to  $E_{MCA}$  stems from spin-orbit interaction across spin-up and spin-down bands.

In conclusion, we found that the Mn monolayer becomes ferromagnetic on the Nb(001) surface, primarily due to Mn-Nb hybridization and the large induced magnetic moment at the Nb surface. Furthermore, Mn/Nb(001) has an in-plane easy axis because the negative shape anisotropy energy overwhelms the small positive magnetocrystalline anisotropy energy. We hope our *ab initio* results stimulate experimental interest in of verification.

- 
- <sup>1</sup>A. J. Freeman and R. Q. Wu, *J. Magn. Magn. Mater.* **100**, 497 (1991).
- <sup>2</sup>M. T. Butterfield, M. D. Crapper, and V. R. Dhanak, *Phys. Rev. B* **66**, 165414 (2002).
- <sup>3</sup>Yoshiki Yonamoto, Toshihiki Yokoyama, Kenta Amemiya, Daiju Matsumura, and Toshiaki Ohta, *Phys. Rev. B* **63**, 214406 (2001).
- <sup>4</sup>T. Igel, R. Pfandzelter, and H. Winter, *Phys. Rev. B* **58**, 2430 (1998).
- <sup>5</sup>D. A. Tulchinsky, J. Unguris, and R. J. Celotta, *J. Magn. Magn. Mater.* **212**, 91 (2000).
- <sup>6</sup>R. Wu and A. J. Freeman, *Phys. Rev. B* **51**, 17131 (1995).
- <sup>7</sup>W. L. O’Brien and B. P. Tonner, *Phys. Rev. B* **51**, 617 (1995).
- <sup>8</sup>B.-Ch. Choi, P. J. Bode, and J. A. C. Bland, *J. Appl. Phys.* **85**, 5063 (1999).
- <sup>9</sup>S. Pick and C. Demangeat, *Surf. Sci.* **584**, 146 (2005).
- <sup>10</sup>S. Blügel, M. Weinert, and P. H. Dederichs, *Phys. Rev. Lett.* **60**, 1077 (1988).
- <sup>11</sup>P. Krüger, M. Taguchi, and S. Meza-Aguilar, *Phys. Rev. B* **61**, 15277 (2000).
- <sup>12</sup>B. Belhadji, S. Lounis, M. Benakki, and C. Demangeat, *Phys. Rev. B* **69**, 064431 (2004).
- <sup>13</sup>M. Bode, S. Heinze, A. Kubetzka, O. Pietzsch, M. Hennefarth, M. Getzlaff, R. Wiesandanger, X. Nie, G. Bihlmayer, and S. Blügel, *Phys. Rev. B* **66**, 014425 (2002).
- <sup>14</sup>B.-Ch. Choi, P. J. Bode, and J. A. C. Bland, *Phys. Rev. B* **58**, 5166 (1998).
- <sup>15</sup>B. K. Rao and P. Jena, *Phys. Rev. Lett.* **89**, 185504 (2002).
- <sup>16</sup>Jisang Hong and R. Q. Wu (unpublished).
- <sup>17</sup>H. J. Lee, W. Ho, and M. Persson, *Phys. Rev. Lett.* **92**, 186802 (2004).
- <sup>18</sup>Jisang Hong, D. S. Wang, and R. Q. Wu, *Phys. Rev. Lett.* **94**, 137206 (2005).
- <sup>19</sup>P. Ferriani, S. Heinze, G. Bihlmayer, and S. Blügel, *Phys. Rev. B* **72**, 024452(R) (2005).
- <sup>20</sup>M. Weinert, E. Wimmer, and A. J. Freeman, *Phys. Rev. B* **26**, 4571 (1982).
- <sup>21</sup>J. P. Perdew, K. Burke, and M. Ernzerhof, *Phys. Rev. Lett.* **77**, 3865 (1996).
- <sup>22</sup>Ruqian Wu and A. J. Freeman, *Phys. Rev. Lett.* **73**, 1994 (1994).
- <sup>23</sup>M. Altarelli, *Phys. Rev. B* **47**, 597 (1993).
- <sup>24</sup>X. Wang, R. Wu, D. S. Wang, A. J. Freeman, *Phys. Rev. B* **54**, 61 (1996).